Available online at www.sciencedirect.com

SCIENCE DIRECT

Biochimica et Biophysica Acta 1664 (2004) 161–171

BIOCHIMICA ET BIOPHYSICA ACTA
BBA

www.bba-direct.com

Membrane properties of plant sterols in phospholipid bilayers as determined by differential scanning calorimetry, resonance energy transfer and detergent-induced solubilization

Katrin K. Halling*, J. Peter Slotte

Department of Biochemistry and Pharmacy, Åbo Akademi University, P.O. Box 66, FIN 20521 Turku, Finland

Received 16 March 2004; accepted 11 May 2004
Available online 9 June 2004

Abstract

The increased use of plant sterols as cholesterol-lowering agents warrants further research on the possible effects of plant sterols in membranes. In this study, the effects of the incorporation of cholesterol, campesterol, β-sitosterol and stigmasterol in phospholipid bilayers were investigated by differential scanning calorimetry (DSC), resonance energy transfer (RET) between *trans* parinaric acid (tPA) and 2-(6-(7-nitrobenz-2-oxa-1,3-diazol-4-yl)amino)hexanoyl-1-hexadecanoyl-*sn*-glycero-3-phosphocholine (NBD-PC), and Triton X-100-induced solubilization. The phospholipids used were 1,2-dipalmitoyl-*sn*-glycero-3-phosphocholine (DPPC), D-*erythro*-*N*-palmitoyl-sphingomyelin (PSM), and 1-palmitoyl-2-oleoyl-*sn*-glycero-3-phosphocholine (POPC). In DSC experiments, it was demonstrated that the sterols differed in their effect on the melting temperatures of both the sterol-poor and the sterol-rich domains in DPPC and PSM bilayers. The plant sterols gave rise to lower temperatures of both transitions, when compared with cholesterol. The plant sterols also resulted in lower transition temperatures, in comparison with cholesterol, when sterol-containing DPPC and PSM bilayers were investigated by RET. In the detergent solubilization experiments, the total molar ratio between Triton X-100 and POPC at the onset of solubilization ($R_{t,sat}$) was higher for bilayers containing plant sterols, in comparison with membranes containing cholesterol. Taken together, the observations presented in this study indicate that campesterol, β-sitosterol and stigmasterol interacted less favorably than cholesterol with the phospholipids, leading to measurable differences in their domain properties.

Keywords: Campesterol; Stigmasterol; Sitosterol; Phosphatidylcholine; Sphingomyelin; Membrane heterogeneity

1. Introduction

Sterols are essential components in the membranes of eukaryotic cells. In mammalian cell membranes, cholesterol is the main sterol. It often constitutes around one third of the total lipid mass of the plasma membrane [1]. The membranes of the Golgi apparatus contain less cholesterol than the plasma membrane, but more than the membranes of the mitochondria and the endoplasmic reticulum [2]. While the hydrophobic effect drives the formation of the bilayer, attractive van der Waals forces constitute the primary interactions between the phospholipid acyl chains and between the phospholipid acyl chains and cholesterol [3]. In addition to the van der Waals forces, the interactions between cholesterol and phospholipids may involve hydrogen bonds between the hydroxyl group of cholesterol and the interfacial groups of the phospholipids [4–6]. Cholesterol seems to interact more favorably with sphingomyelins than with, e.g. phosphatidylcholines (reviewed in Ref. [4]), which has been anticipated to promote the formation of lateral domains in cellular membranes [7,8]. Incorporation of increasing amounts of cholesterol into pure bilayers of many naturally occurring phospholipids induces the forma-

Abbreviations: DPPC, 1,2-dipalmitoyl-*sn*-glycero-3-phosphocholine; DSC, differential scanning calorimetry; NBD-PC, 2-(6-(7-nitrobenz-2-oxa-1,3-diazol-4-yl)amino)hexanoyl-1-hexadecanoyl-*sn*-glycero-3-phosphocholine; POPC, 1-palmitoyl-2-oleoyl-*sn*-glycero-3-phosphocholine; PSM, D-*erythro*-*N*-palmitoyl-sphingomyelin; RET, resonance energy transfer; $R_{t,sat}$, total molar ratio of detergent to phospholipid at the onset of solubilization; tPA, *trans* parinaric acid

* Corresponding author. Tel.: +358-2-215-4268; fax: +358-2-215-4010.
E-mail address: katrin.halling@abo.fi (K.K. Halling).

0005-2736/$ - see front matter © 2004 Elsevier B.V. All rights reserved.
doi:10.1016/j.bbamem.2004.05.006

tion of a liquid-ordered phase [9], and gradually abolishes the liquid-crystalline and gel phases (e.g. Refs. [10,11]). In the liquid-ordered phase, the phospholipid acyl chains are extended and relatively tightly packed. There is, nevertheless, a relatively high degree of translational motion in the plane of the bilayer [12].

A small fraction of cholesterol can be found in the membranes of some plant cells [13]. However, for the most part, the sterol content of plant cell membranes is made up by other sterols, e.g. campesterol, β-sitosterol and stigmasterol (for structures, see Fig. 1). These and several other sterols, with a widespread occurrence in plant cell membranes, differ structurally from cholesterol only with regard to their side chain. Campesterol has a methyl group at carbon 24, while β-sitosterol and stigmasterol have an ethyl group in this position. Stigmasterol furthermore contains an additional *trans* double bond between carbons 22 and 23. Carbon 24 in campesterol and β-sitosterol has R chirality, while the equivalent carbon in stigmasterol has S chirality due to the *trans* configuration of the side chain double bond [14,15].

It has been established that several plant sterols, plant stanols and conjugates of these induce a decrease in the serum total and low-density lipoprotein cholesterol level, which in turn may cause suppression of atherogenesis (reviewed in, e.g. Ref. [16]). The mechanisms for the decrease in cholesterol concentration related to plant sterols (stanols) are still not completely understood, but it is clearly demonstrated that the effect to a large part is based on the plant sterols and stanols reducing the rate of intestinal cholesterol absorption [17]. Plant sterols are absorbed from the intestine to a lower extent in comparison to cholesterol [18]. Nevertheless, when absorbed, plant sterols are transported in lipoproteins and may get incorporated in cellular membranes [19–22]. A change in sterol content could be critical for the membrane functions of erythrocytes, which lack the ability to adjust the sterol content of their plasma membrane [23,24].

There are several studies that have explored the effects of plant sterols in phospholipid membranes, such as effects on phospholipid condensation [25], membrane permeability to small solutes [26,27], phospholipid order [28–30], membrane interfacial qualities [31], the thermotropic properties of phospholipid bilayers [32], and on membrane domains [33]. Further research is, however, warranted in order to better understand the properties of sterol-rich domains in plant sterol-containing phosphatidylcholine and sphingomyelin systems. In our study, we have applied differential scanning calorimetry (DSC), resonance energy transfer (RET) and detergent solubilization detected by light scattering, in comparing the properties of cholesterol, campesterol, β-sitosterol and stigmasterol in phospholipid bilayers. By using well-defined model membrane systems, we have gained information on what effect an alkyl substituent and a double bond in cholesterol side chain have on the interactions between the sterol molecule and the phospholipids of the host bilayer. Knowledge of the properties of plant sterols in lipid model membranes improves our understanding on what effects the incorporation of plant sterols into cellular membranes may have.

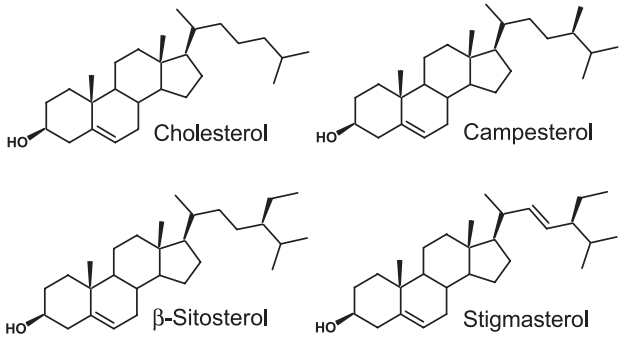

Fig. 1. Molecular structures of the sterols included in the study.

2. Materials and methods

2.1. Materials

Cholesterol, campesterol, β-sitosterol and stigmasterol were purchased from Sigma Chemicals (St. Louis, MO, USA). The concentrations of the sterol stock solutions were determined from monolayer isoterms. The calculations were based on a mean molecular area of 38.5 $Å^2$ (cholesterol and campesterol) or 39.5 $Å^2$ (β-sitosterol and stigmasterol) at the collapse of the monolayer. The 1,2-dipalmitoyl-*sn*-glycero-3-phosphocholine (DPPC) and 1-palmitoyl-2-oleoyl-*sn*-glycero-3-phosphocholine (POPC) were obtained from Avanti Polar Lipids (Alabaster, AL, USA). D-*erythro*-*N*-Palmitoyl-sphingomyelin (PSM) was purified from egg yolk sphingomyelin (Avanti Polar Lipids) by reverse phase high performance liquid chromatography (HPLC; LiChrospher 100 RP-18 column, 5 μm particle size, column dimensions 250 × 4 mm) using methanol as eluent (at 5 ml/min, column temperature 40 °C). The identity of the product was verified by mass spectroscopy (Micromass Quattro II, Manchester, UK). *trans* Parinaric acid (tPA—kindly provided by Dr. Somerharju) and 2-(6-(7-nitrobenz-2-oxa-1,3-diazol-4-yl)amino)hexanoyl-1-hexadecanoyl-*sn*-glycero-3-phosphocholine (NBD-PC), both from Molecular Probes (Eugene, OR, USA), were stored at − 87 °C until solubilized in methanol and ethanol, respectively. Stock solutions were used within a week and stored at − 20 °C. The purity of the probes was analyzed by HPLC (LiChrospher 100 RP-18 column, 5 μm particle size, column dimensions 125 × 4 mm) before use. The probes were found to be 99% pure. The eluent for the tPA analysis was 20 vol.% water in methanol, while pure methanol was used for NBD-PC. The water was purified by reverse osmosis followed by passage through a Millipore UF Plus water purification system, to yield a product with a resistivity of 18.2 MΩ cm.

2.2. DSC

Bilayer vesicles were prepared from DPPC or PSM together with 0, 5, 10, 15, 20 or 25 mol% sterol. The lipids were dried, first under nitrogen and then in vacuum for a minimum of 8 h. The dry lipids were stored at −20 °C for a maximum of 8 days. Prior to the experiments, the lipids were heated to 50 °C before 1 ml of 50 °C water was added. The final phospholipid concentration was 1.4 mM. The lipid suspensions were vortexed and sonicated in a Bransonic 2510E-MT bath sonicator (Branson Ultrasonics, Danbury, LT, USA) for 4 min at 50 °C. The vesicle suspensions were then cooled to room temperature and analyzed using a Nano II high-sensitivity scanning calorimeter (Calorimetric Science Corporation, Provo, UT, USA). The reference cell contained water. Heating scans from 10 to 60 or 70 °C at a scan rate of 0.5 °C/min were obtained. When the endotherm shape indicated the presence of more than one main transition component, the endotherm was deconvoluted. This procedure gave rise to one broad and one sharp component, representing the melting of sterol-rich and sterol-poor domains, respectively [10,34,35]. The deconvolution was performed using Origin 6.0 Peak Fitting software (Microcal Software, Northampton, MA, USA).

2.3. RET

Based on the fact that the emission wavelength spectra of tPA overlaps the excitation wavelength spectra of NBD-PC, we applied the two probes as a RET pair. tPA, used here as a RET donor, partitions favorably into the lamellar gel phase of a bilayer, where its quantum yield is higher than in the less tightly packed liquid-crystalline phase [36,37]. Accordingly, the thermal transition from lamellar gel to liquid-crystalline phase in single-component phospholipid bilayers can be detected as a decrease in fluorescence intensity. NBD-PC, the acceptor in our RET setup, preferentially resides in the disordered liquid phases [38,39], or in packing defects when no liquid phase is present [40]. The highest quantum yield of NBD-PC in 1,2-dimyristoyl-*sn*-glycero-3-phosphocholine and DPPC bilayers is reached in the gel and liquid-crystalline coexistence region [41].

Vesicles were prepared from DPPC or PSM together with sterol, tPA and NBD-PC. The molar ratios of tPA and NBD-PC to phospholipid were 1:1000 and 1:80, respectively [42]. The amount of sterol included was 0, 5, 10, 15, 20 or 25 mol% of the total amount of lipid. The lipids were dried under nitrogen, resuspended in water to a final phospholipid concentration of 0.05 mM, heated to 50 °C and sonicated for 2 min in a Branson probe sonifier W-250 (Branson Ultrasonics; 20% duty cycle, power output 30 W). The fluorescent probes were protected from light during the procedures. All solvents used together with tPA were saturated with argon before use, to minimize the risk of oxidation. The fluorescence measurements were performed on a PTI QuantaMaster 1 fluorimeter (Photon Technology International, Lawrenceville, NJ, USA), with both the excitation and emission slits set to 5 nm. The excitation and emission wavelenghs were set to 306 nm (excitation of tPA) and 530 nm (emission of NBD-PC), respectively. The temperature was controlled by a Peltier element, with a temperature probe immersed in the sample solutions. For every sterol concentration, two to four separately prepared vesicle suspensions were analyzed. Heating scans were recorded for the temperature interval 17 to 65 °C, at a scan rate of 5 °C/min. To determine the dependence of the RET efficiency/temperature plots on the scan rate, heating scans were obtained at a scan rate of 1 °C/min as well. No qualitative differences were observed between heating scans obtained at the two different scan rates. To check the possible importance of vesicle preparation procedure, experiments were performed on vesicle suspensions prepared according to the procedure applied for the DSC experiments. No differences were observed between the RET efficiency/temperature plots obtained from vesicles prepared according to the different protocols (bath vs. probe sonication). Quartz cuvettes were used for the experiments and the sample solutions were kept at constant stirring (260 rpm) during the measurements.

2.4. Bilayer solubilization by Triton X-100 as detected by light scattering measurements

Vesicle suspensions were prepared from POPC and sterol (33 mol% of total lipid content). The lipids were dried under nitrogen, resuspended in buffer (10 mM Tris, 140 mM NaCl, pH 7.4) to a final phospholipid concentration of 0.5 mM, vortexed and sonicated for 15 min in a Bransonic 2510E-MT bath sonicator at room temperature. The experiments were performed using a PTI Quantamaster 1 spectrofluorimeter with both the excitation and emission slits set to 5 nm. The excitation and emission wavelengths were set to 400 nm. The experiments were performed by injecting 5-μl aliquots of a Triton X-100 solution (10 mM, in buffer) into a quartz cuvette initially containing 1.5 ml of vesicle suspension. When the intensity of the scattered light started decreasing, as a sign of the formation of mixed micelles (i.e. solubilization; [43]), 20-μl aliquots of the same Triton X-100 solution were added to reach complete solubilization. In our control experiments, the Triton X-100 solution was replaced with buffer. The sample solutions were kept at constant stirring (260 rpm) during the measurements. All experiments were carried out at 22 ± 1 °C.

3. Results

3.1. The effect of sterols on the phase transitions of DPPC and PSM bilayers

We used DSC to study the effect of sterol on the transition from lamellar gel to liquid-crystalline phase in

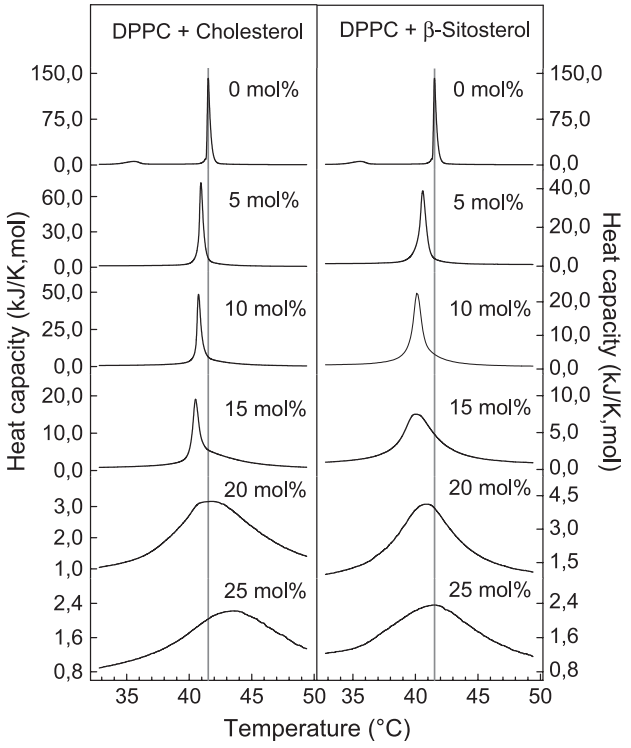

Fig. 2. Representative DSC thermograms of DPPC bilayers containing cholesterol or β-sitosterol. The figure presents heating scans obtained with a phospholipid concentration of 1.4 mM and a scan rate of 0.5 °C/min. The vertical reference line indicates the main transition temperature (41.6 °C) of pure DPPC bilayers.

DPPC and PSM bilayers. In the endotherm of the pure DPPC bilayers, two peaks, representing the pretransition (35.5 °C) and the main transition (41.6 °C), were observed (Fig. 2). The enthalpy of the main transition amounted to 38.4 kJ/mol. These values are in accordance with previously reported results [44]. A detectable pretransition was also present in the endotherm of DPPC bilayers containing 5 mol% sterol (not seen in Fig. 2 due to the selected *y*-axis scale). At 10 mol% sterol, no pretransition was observed. This is in line with results reported by e.g. McMullen et al. [10], who showed that the pretransition of DPPC bilayers is abolished at a cholesterol concentration of 5 to 6 mol%. Campesterol, β-sitosterol and stigmasterol seemed to abolish the pretransition at approximately the same concentration as cholesterol. On the whole, all sterols seemed to have a similar effect on the pretransition and the main transition of DPPC bilayers. The main transition enthalpy was gradually reduced, and the cooperativity of the transition decreased with increasing sterol concentration (this trend has previously been reported for cholesterol-containing phosphatidylcholine bilayers in Refs. [10,32,34], and for plant sterol-containing DPPC bilayers in Ref. [32]). In Fig. 2, the endotherms representing the transition of cholesterol- and β-sitosterol-containing DPPC bilayers are shown. Due to space limitations, and their close resemblance to the endotherms of cholesterol- and β-sitosterol-containing bilayers, the endotherms of the melting of campesterol- and stigmasterol-containing bilayers are not shown.

In the analysis of the main phase transition, we deconvoluted the main transition endotherm obtained for DPPC bilayers containing 5, 10 or 15 mol% sterol. The deconvolution gave rise to one sharp and one broad component, previously described to represent the melting of sterol-poor and sterol-rich domains, respectively (deconvolutions not shown) [10,34]. At sterol concentrations of 20 or 25 mol%, only the broad component was clearly detected. In most cases, an increase in sterol concentration brought about a decrease in the temperature of the sharp component (Fig. 3A). In contrast, the temperature of the broad component increased with sterol concentration (Fig. 3B). The sterols differed in their effect on the temperature of both the sharp and the broad component. The temperatures of both components for all the studied mole fractions were highest in bilayers containing cholesterol. The presence of any of the other sterols resulted in lowered temperatures in the following order: campesterol>stigmasterol>β-sitosterol. This suggests that the plant sterols have a lower ability to stabilize and to order the DPPC bilayer compared to cholesterol.

The melting of pure PSM bilayers gave rise to an endotherm with two peaks, a pretransition at 27.4 °C (not shown) and a main phase transition at 40.6 °C (Fig. 4). The enthalpy of the main transition was 33.9 kJ/mol. These results are in accordance with results from previous reports

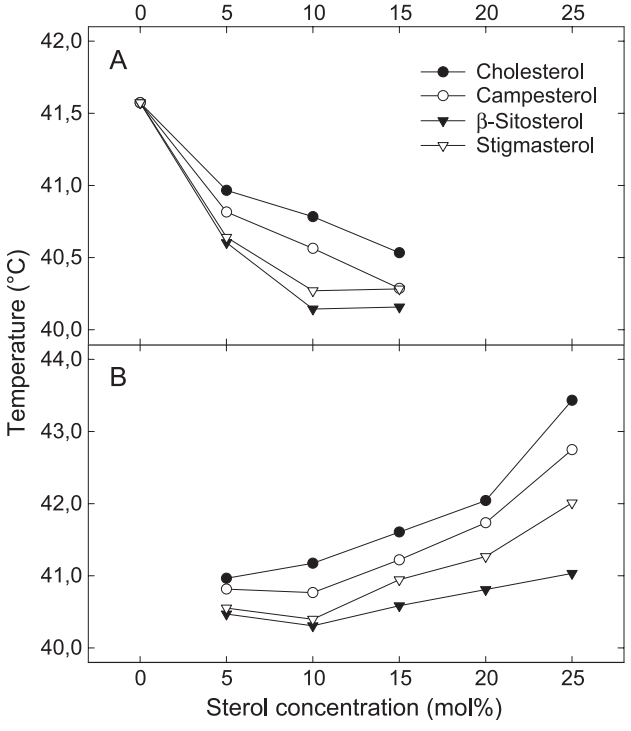

Fig. 3. The temperature of the sharp (A) and the broad (B) component of the main phase transition as a function of sterol concentration in DPPC bilayers. The sharp and the broad component (representing the melting of sterol-poor and sterol-rich domains, respectively) were the result of the deconvolution of the overall endotherms obtained by DSC.

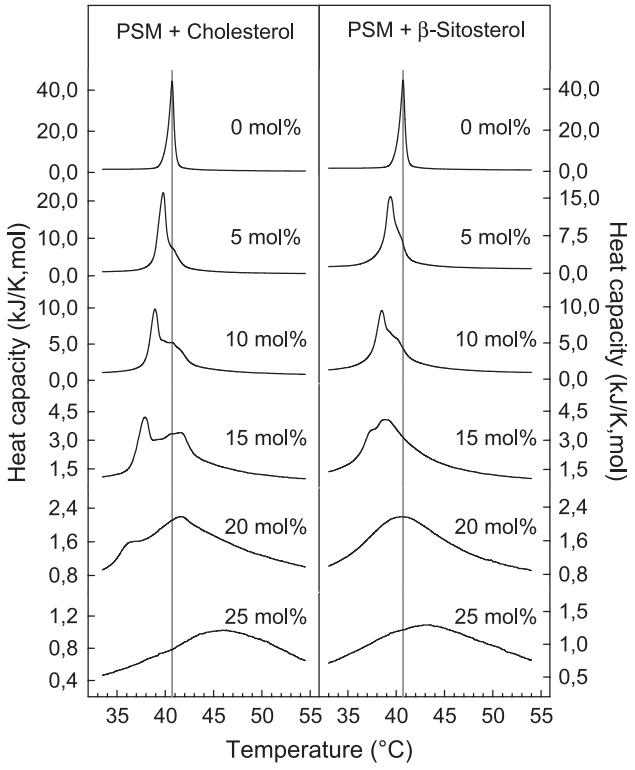

Fig. 4. Representative DSC thermograms of PSM bilayers containing cholesterol or β-sitosterol. The heating scans presented in the figure were obtained with a phospholipid concentration of 1.4 mM and a scan rate of 0.5 °C/min. The vertical reference line indicates the main transition temperature (40.6 °C) of pure PSM bilayers.

[45–47]. The pretransition was still clearly visible at 5 mol% sterol (not shown). As previously reported, the pretransition of PSM bilayers shifted to higher temperatures when the sterol concentration was raised from 0 to 5 mol% [47]. This is contrary to the behavior of the pretransition of DPPC bilayers. All sterols appeared to have a similar effect on the pretransition and the main transition of PSM bilayers. The main transition enthalpy was reduced, and the cooperativity of the main transition decreased with increasing sterol concentration. The endotherms recorded for PSM bilayers containing cholesterol and β-sitosterol are shown in Fig. 4. The equivalent endotherms of campesterol- and stigmasterol-containing PSM bilayers were similar and are not shown.

The main transition endotherm was deconvoluted when its shape indicated the presence of more than one component (not shown) [35]. The deconvolution resulted in two clearly discernible components, a sharp (sterol-poor) and a broad one (sterol-rich), in bilayers containing 5–15 mol% sterol. In bilayers containing 20 mol% cholesterol or campesterol, a small shoulder on the endotherm at a temperature around 37 °C indicated the presence of a sharp component next to the broad one. Because of the small size of the sharp component, it could not be subtracted from the overall endotherm very accurately in the campesterol system. The temperature of the sharp component decreased linearly with increasing concentration of any of the sterols (Fig. 5A). At most mole fractions, the plant sterols seemed to result in slightly lower transition temperatures of the sharp component, as compared with cholesterol. The impact on the temperature of the broad component differed markedly between the sterols (Fig. 5B). Cholesterol gave rise to an increased transition temperature when the sterol concentration was increased from 5 to 15 mol%. Campesterol did not cause any significant change in transition temperature, whereas β-sitosterol and stigmasterol gave rise to a decrease in transition temperature when the amount of sterol was increased from 5 to 15 mol%. When the sterol concentration was increased to 20 and 25 mol%, all sterols caused a rise in transition temperature. The relatively low transition temperatures of the plant sterol-containing PSM bilayers suggest that the plant sterols do not interact as favorably as cholesterol with PSM.

3.2. RET between tPA and NBD-PC in DPPC and PSM bilayers

We performed RET measurements to investigate the effect of the different sterols on domain formation in DPPC and PSM bilayers. Björkqvist and Slotte recently studied the

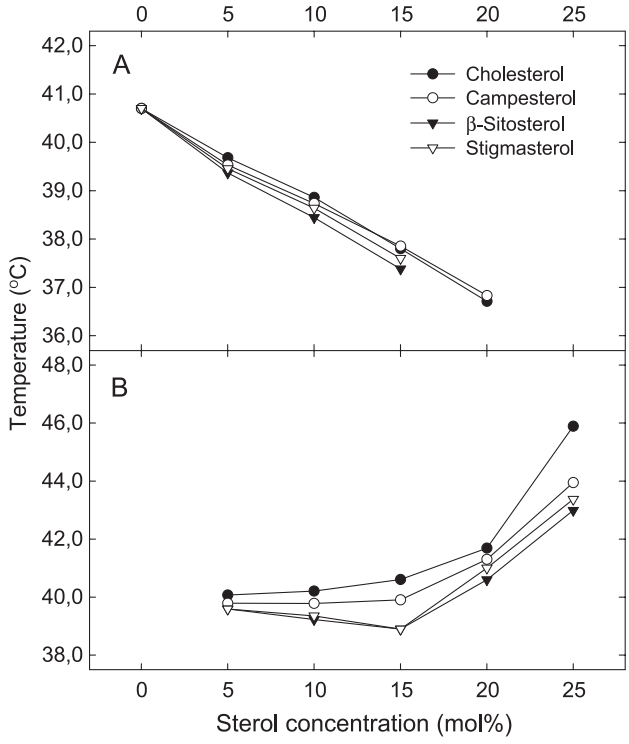

Fig. 5. The temperature of the sharp (A) and the broad (B) component of the main phase transition observed in the endotherm of sterol-containing PSM bilayers. The sharp and the broad component (representing the melting of sterol-poor and sterol-rich domains, respectively) were the result of the deconvolution of the overall endotherms obtained by DSC. At 20 mol% campesterol, only a small shoulder in the endotherm indicated the presence of a sharp transition component. It was therefore not possible to determine the temperature of the component very accurately.

domain forming properties of cholesterol in DPPC and PSM bilayers, applying this experimental setup (Björkqvist, J. and Slotte, J.P., 2004, unpublished data). When sterol-free DPPC bilayers were analyzed in the present study, the RET efficiency started to increase at a temperature around 32 °C and peaked at approximately 42.4 °C (Fig. 6). The increased RET efficiency probably reports on the pretransition and main transition of the pure phospholipid bilayer. Representative RET efficiency/temperature plots, which were obtained for DPPC together with different amounts of cholesterol or β-sitosterol, are shown in Fig. 6. RET efficiency/temperature plots of DPPC bilayers containing campesterol and stigmasterol are not shown due to their close resemblance to the RET efficiency/temperature plots obtained for cholesterol and β-sitosterol-containing bilayers. At up to 15 mol% sterol, the RET efficiency maximum for all sterols occurred at temperatures close to the transition temperature of sterol-poor domains, as seen in our DSC experiments. At higher sterol concentrations, the temperature for maximal RET efficiency decreased more in the β-sitosterol- and stigmasterol-containing bilayers than in the cholesterol- and campesterol-containing bilayers. This indicates that the domain stability and/or probe distribution was different in the DPPC bilayer systems investigated in this study.

The main features of the RET efficiency/temperature plots of PSM bilayers (Fig. 7, results for campesterol and stigmasterol not shown) differed somewhat from the plots obtained from DPPC bilayers. At low sterol concentration (5 to 15 mol%), a RET efficiency minimum and a RET efficiency maximum were clearly observed in PSM membranes containing cholesterol, campesterol, β-sitosterol or stigmasterol. The RET efficiency minimum, which was particularly marked in cholesterol-containing PSM bilayers, most likely resulted from transient quenching of the fluorescence from NBD-PC, due to an enrichment of NBD-PC to a domain boundary during the transition (Björkqvist, J. and Slotte, J.P., 2004, unpublished data). The RET efficiency maxima occurred at temperatures higher than those observed for both the sharp and the broad transition components using DSC. This probably reflects how PSM can influence the lateral distribution of the probes used in this study (for a general discussion on this phenomena, see Ref. [48]). The RET efficiency/temperature plots for sterol-containing PSM bilayers again showed that at higher sterol concentration, the temperature for maximal RET efficiency was lower with β-sitosterol and stigmasterol than with cholesterol or campesterol, indicating differences in domain stability in the different PSM bilayer systems.

To visualize the differences in the effect of the sterols on the RET efficiency in more detail, the temperatures of the

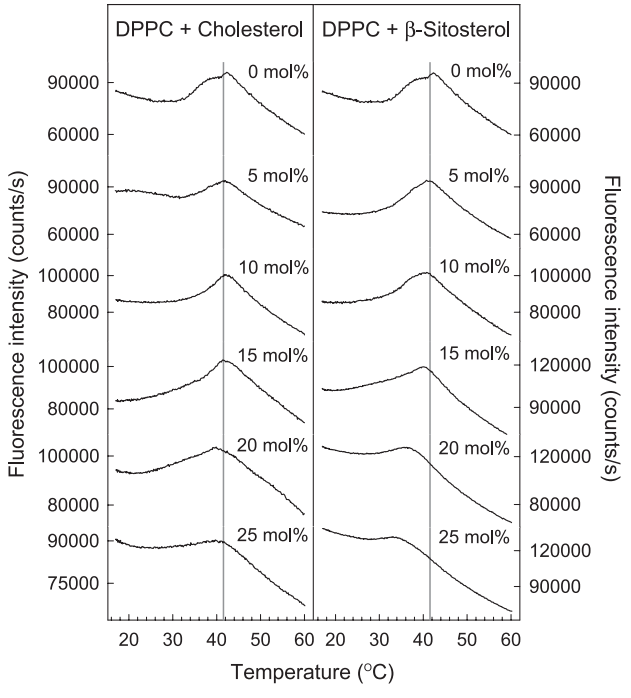

Fig. 6. RET between tPA and NBD-PC in cholesterol- and β-sitosterol-containing DPPC bilayers. The RET efficiency, measured as the emission intensity of NBD-PC, is presented as a function of temperature. The experiments were performed at a scan rate of 5 °C/min. The vertical reference line indicates the main transition temperature (41.6 °C) of pure DPPC bilayers.

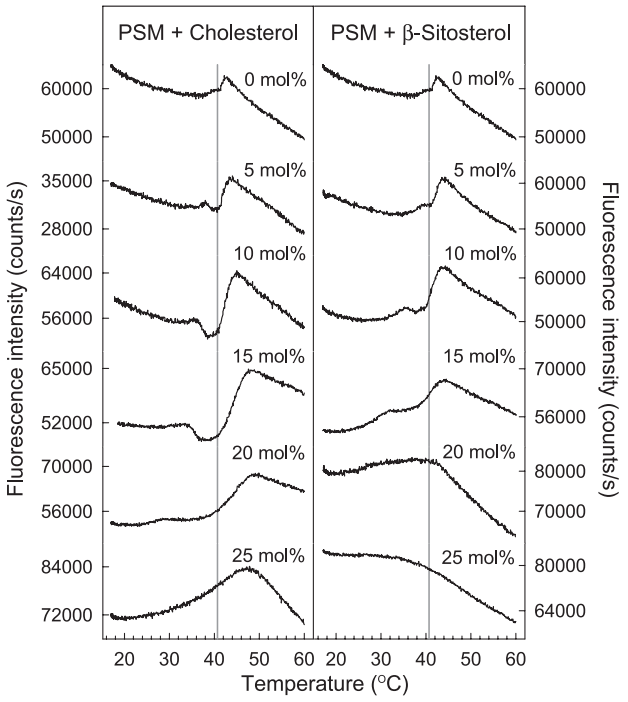

Fig. 7. RET between tPA and NBD-PC in cholesterol- or β-sitosterol-containing PSM bilayers. The RET efficiency, measured as the emission intensity of NBD-PC, is presented as a function of temperature. The RET efficiency/temperature plot of PSM bilayers containing 5 mol% cholesterol was recorded with instrumental settings that differed from the settings used in the other experiments. Hence, the measured counts per second (cps) should not be directly compared with the values obtained for other samples. The vertical reference line indicates the main transition temperature (40.6 °C) of pure PSM bilayers.

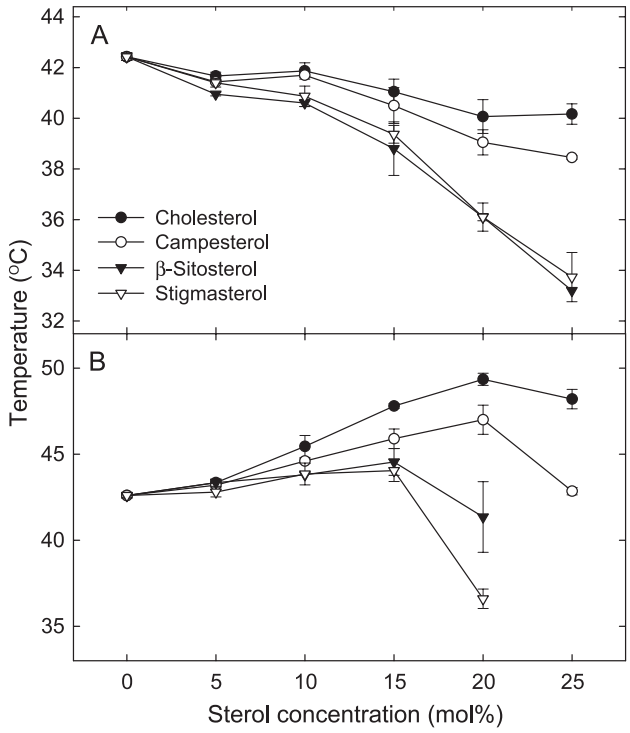

Fig. 8. The temperature of the RET efficiency maximum in tPA- and NBD-PC-containing DPPC (A) and PSM (B) bilayers, plotted as a function of sterol concentration. The temperatures were derived from results presented in Figs. 6 and 7.

RET efficiency maxima were plotted as a function of sterol concentration (Fig. 8). The RET efficiency maximum of the sterol-containing DPPC bilayers shifted to lower temperatures with increasing sterol concentration (Fig. 8A). With an increasing amount of cholesterol, the RET efficiency peak temperature decreased and reached approximately 40 °C at 25 mol% cholesterol. The effect of campesterol on the RET efficiency was very similar to that of cholesterol. β-Sitosterol and stigmasterol gave rise to a relatively large shift in RET efficiency peak temperature, compared with both cholesterol and campesterol. At 25 mol% sterol, the RET efficiency maximum was observed at about 33 °C. The sterol-dependent temperature shift of the RET efficiency maximum seemed to correlate with the shift of the transition onset temperature of sterol-poor domains, as measured in the DSC experiments (not shown).

The temperature at which the RET efficiency was maximal in sterol/PSM bilayers is plotted as a function of sterol concentration in Fig. 8B. Cholesterol gave rise to the largest increase in peak temperature. At 20 mol% cholesterol, the RET efficiency peak was seen at approximately 49 °C. The increase in RET efficiency peak temperature caused by campesterol was more modest, reaching approximately 47 °C at 20 mol%. At 25 mol%, the RET efficiency peak temperature of both cholesterol- and campesterol-containing PSM bilayers was lower than at 20 mol%. In β-sitosterol- and stigmasterol-containing PSM bilayers the maximal RET efficiency peak temperature (about 44 °C) was measured at 15 mol% sterol.

3.3. Solubilization of POPC bilayers by Triton X-100

We investigated the detergent resistance of sterol-free and sterol-containing POPC vesicles to obtain information about possible differences in the effect of the sterols on the bilayer stability. To detect the onset of solubilization, we monitored the light scattering of the vesicle suspensions. In the experiments, 5-μl aliquots of a 10 mM Triton X-100 solution were injected into a suspension of vesicles composed of POPC, or of POPC together with sterol (33 mol%). The intensity of the scattered light was noted after each addition (Fig. 9). In analyzing the experimental data, we focused on the ratio of the total amount of Triton X-100 to POPC at the onset of solubilization ($R_{t,sat}$). The $R_{t,sat}$ value measured for sterol-free vesicles was 0.74. When the bilayers contained cholesterol, the lowest $R_{t,sat}$ (0.61) was obtained. The plant sterols caused higher $R_{t,sat}$ values in the following order: campesterol (0.65) < β-sitosterol (0.77) < stigmasterol (0.82). Four to six measurements on at least two separately prepared vesicle suspensions were performed with every bilayer composition. The standard deviation of the measured $R_{t,sat}$ values for each bilayer composition was less than 3%. We speculate that the higher $R_{t,sat}$ values observed for plant sterol-containing membranes are due to less favorable interactions between the sterol and phospholipid molecules. The sterol-free vesicle suspensions all showed an initial increase in light scattering intensity, most likely as a result of vesicle growth and/or fusion [49]. The light scattering intensity of sterol-containing samples prior to $R_{t,sat}$ did not, however, follow a reproducible pattern.

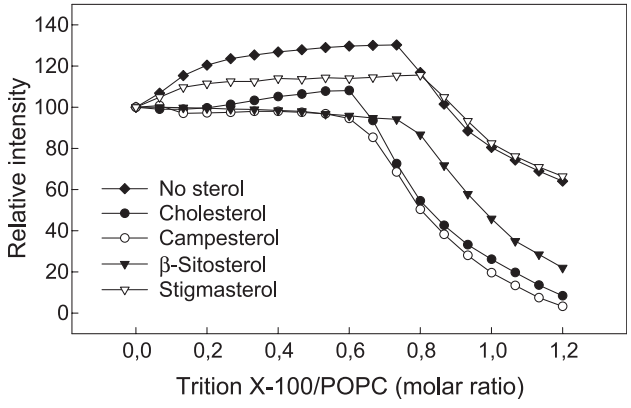

Fig. 9. The onset of Triton X-100-induced solubilization of sterol-free and sterol-containing POPC vesicles (representative plots). Aliquots (5 μl) of a 10 mM Triton X-100 solution were injected into a cuvette initially containing 1.5 ml of vesicle suspension. The initial phospholipid concentration was 0.5 mM. The intensity of the scattered light was determined subsequent to every injection and the measured values were normalized to the initial intensity (100%).

4. Discussion

4.1. The main transition of sterol-containing DPPC and PSM bilayers

We recorded and analyzed DSC thermograms of bilayers composed of pure DPPC and PSM, and of binary mixtures of DPPC or PSM together with cholesterol, campesterol, β-sitosterol or stigmasterol. This was carried out to study possible differences in the ability of the sterols to influence the thermotropic behavior of DPPC and PSM bilayers. The enthalpy and the temperature of both the pretransition and the main transition of the pure DPPC and PSM bilayers correlated well with previously reported results (phosphatidylcholine data reviewed in Ref. [44], sphingomyelin data (racemic D-*erythro*/L-*threo* mixtures) reviewed in Ref. [45], D-*erythro* sphingomyelin data reported in Refs. [46,47]). All plant sterols seemed to abolish the pretransition of DPPC and PSM bilayers at similar concentrations as cholesterol. This is in line with the results reported by McMullen et al. [50], who studied the pretransition of DPPC bilayers in the presence of cholesterol and androstenol (a cholesterol analogue with no side chain). McMullen and co-workers noted that a C17 side chain was not important for the ability of the sterol to abolish the pretransition of DPPC.

In our DSC experiments, the major difference that was observed between cholesterol, campesterol, β-sitosterol and stigmasterol was their different effects on the temperatures of both the sharp and the broad component (representing the melting of sterol-poor and sterol-rich domains, respectively [10,34,35]) in DPPC and PSM bilayers. Compared with cholesterol, the plant sterols gave rise to lower transition temperatures of both components. A high transition temperature probably indicates the presence of relatively favorable, stabilizing interactions between the sterols and the phospholipid molecules constituting the bilayer [10]. Thus, our DSC results suggest that campesterol interacts with DPPC and PSM less favorably than cholesterol, due to its additional methyl group. Stigmasterol and β-sitosterol, both having an ethyl group in their side chain, seem to interact even less favorably than campesterol with DPPC and PSM. A comparison between bilayers containing β-sitosterol and stigmasterol suggests that the double bond at carbon 22 gives stigmasterol a slightly higher ability to favorably interact with DPPC. This agrees with the results recently presented by Bernsdorff and Winter [51], who studied the molecular order of sterol-containing DPPC bilayers, by measuring the steady-state fluorescence anisotropy of 1-(4-trimethylammonium-phenyl)-6-phenyl-1,3,5-hexatriene. Their results indicated that stigmasterol was slightly more potent than β-sitosterol in ordering the acyl chains of DPPC, considering sterol levels of up to 30 mol% [51]. The ordering effect of both β-sitosterol and stigmasterol was not as high as that of cholesterol, particularly considering high sterol levels (50 mol%) [51]. When McKersie and Thompson [32] applied DSC to study the effect of cholesterol, campesterol, β-sitosterol and stigmasterol on the main transition of DPPC bilayers, they did not see a difference between the effects of the sterols. The divergence between our results and the results of McKersie and Thompson could stem from different vesicle preparation procedures or differences in sensitivity of the DSC instruments used.

Based on the results obtained from our DSC experiments, we speculate that the plant sterols have a lower capacity than cholesterol for packing tightly with DPPC and PSM. This conclusion is in agreement with the results reported by Demel and co-workers [25]. They observed that stigmasterol caused a somewhat lower degree of area condensation in 1-stearoyl-2-oleoyl-*sn*-glycero-3-phosphocholine monolayers than cholesterol. The packing density of a bilayer has also been assessed as a function of the permeability of the bilayer. This approach was chosen by Demel et al. [26] and Yamauchi et al. [27], who showed that the capacity of both β-sitosterol and stigmasterol for reducing the glucose permeability of egg phosphatidylcholine and DPPC vesicles was smaller than the capacity of cholesterol. β-Sitosterol appeared to be slightly more effective, compared with stigmasterol, in reducing the permeability [27]. The DSC results reported in the present study are in good agreement with the observations made in the above permeability studies. Water permeability experiments by Schuler et al. [29], however, indicated that β-sitosterol interacted somewhat more favorably with soybean phosphatidylcholine compared to cholesterol. In the same study, stigmasterol was clearly less effective than cholesterol in reducing water permeability, while a mixture of campesterol and its 24S-epimer, dihydrobrassicasterol, showed a permeability reducing effect which was approximately as large as that of cholesterol. These results correlated well with the different ordering effects of plant sterols in soybean phosphatidylcholine bilayers, as studied by ^{2}H-NMR [29] and 1,6-diphenyl-1,3,5-hexatriene anisotropy [28,29]. The fact that soybean phosphatidylcholine consists of a mixture of relatively unsaturated phosphatidylcholines may explain part of the differences in the ability of the sterols to induce order and tight packing.

4.2. RET between tPA and NBD-PC in sterol-containing DPPC and PSM bilayers

In our RET experiments, we monitored the RET efficiency as a function of temperature to observe possible differences in the effect of the sterols on domain formation in DPPC and PSM bilayers. Previously, similar RET setups in one- [52] and two-component [42,53,54], and in cholesterol-containing [53,55] phospholipid bilayers have been used to study membrane microheterogeneity. A two-donor RET setup was recently reported to effectively detect domain formation in phospholipid bilayers [56].

The overall profiles of the monitored RET efficiency plots presented in this paper indicate that no exceptionally large difference existed between the domains formed in the

presence of the sterols that were included in this study. This argument is in accordance with the results reported by Xu et al. [33] and Xu and London [57], who used fluorescence quenching to investigate the domain forming properties of various sterols. In their experiments, β-sitosterol and stigmasterol induced the formation of domains in DPPC/1-palmitoyl-2-(12-doxyl)stearoyl-*sn*-glycero-3-phosphocholine and brain sphingomyelin/1-palmitoyl-2-(12-doxyl)-stearoyl-*sn*-glycero-3-phosphocholine bilayers to more or less the same extent as cholesterol [33].

The spectrometric data presented in this work furthermore support the results obtained by DSC. The temperature at which the changes in RET efficiency occurred (indicating altered domain properties) appeared to depend on sterol structure and concentration. β-Sitosterol and stigmasterol, the sterols with the bulkiest side chains, induced maximal RET efficiency at lower temperatures, as compared with campesterol and cholesterol. Campesterol, in turn, induced maximal RET efficiency at somewhat lower temperatures than cholesterol. This was more evident in PSM than in DPPC bilayers. We speculate that the differences in temperatures, at which maximal RET efficiency occurred, reflect the different abilities of the sterols to stabilize sterol-enriched domains in DPPC and PSM bilayers.

4.3. Solubilization of sterol-containing POPC bilayers by Triton X-100

In our solubilization studies, we used the ratio between the total amount of detergent and phospholipid at the onset of solubilization ($R_{t,sat}$) as a measure of bilayer stability. The interactions between detergents and membranes are, to a great extent, dependent on the composition of the bilayer, the packing of the bilayer components, the size of the vesicles, and the molecular structure and concentration of the detergent [58]. When a system contains a certain amount of phospholipid bilayers (constituting vesicles of approximately the same size), the onset of solubilization by a detergent largely depends on the ability of the detergent to partition into the bilayer, and on the amount of detergent molecules that may reside in the bilayer without causing solubilization. Sphingomyelin vesicles have previously been reported to be more sensitive than phosphatidylcholine vesicles to solubilization by Triton X-100 [59–61]. It has been suggested that the lower Triton X-100 concentration needed for solubilization of PSM bilayers is due to a higher packing density, and thus to a lower capacity of PSM bilayers to incorporate Triton X-100 molecules [62]. In a similar manner (provided that all sterols included in our experiments interact approximately in the same way with Triton X-100), our results indicate that a higher $R_{t,sat}$ is the result of a lower lateral packing density of the bilayer, and thereby a higher capacity to incorporate Triton X-100 molecules. According to the above argument, the sterols that were included in this study might give rise to different packing densities in POPC bilayers. Cholesterol would in this case cause the tightest packing, followed by the other sterols in the order: campesterol>β-sitosterol>stigmasterol. These findings agree both with the trend seen in our DSC and RET experiments, and with the previously reported results concerning the different effects of the sterols on monolayer density [25] and bilayer permeability [26,27] that were referred to in Section 4.1.

4.4. Conclusion

Based on the results of this study, we conclude that an alkyl substituent at carbon 24, and a double bond between carbon 22 and 23, play an important role in the interaction between sterols and phospholipids. We speculate that the results obtained by DSC, RET and bilayer solubilization point to a sterol-dependent effect on the order and the packing density of a phospholipid bilayer. Our findings gives further support to previously reported results which have indicated that cholesterol, compared to plant sterols, can induce a higher degree of order in bilayers composed of mainly saturated phosphatidylcholines. Our results suggest that plant sterols, if incorporated into membranes of cells, are likely to affect the dynamic properties of sterol-enriched domains. This in turn may interfere with metabolic and functional processes that depend on such domains.

Acknowledgements

We thank Drs. Bodil Ramstedt and Thomas Nyholm for valuable comments and help. This study was supported by generous grants from the National Graduate School of Informational and Structural Biology, the Academy of Finland and the Sigrid Juselius Foundation.

References

[1] Y. Lange, M.H. Swaisgood, B.V. Ramos, T.L. Steck, Plasma membranes contain half the phospholipid and 90% of the cholesterol and sphingomyelin in cultured human fibroblasts, J. Biol. Chem. 264 (1989) 3786–3793.
[2] P.L. Yeagle, Cholesterol and the cell membrane, Biochim. Biophys. Acta 822 (1985) 267–287.
[3] J.N. Israelachvili, Intermolecular and Surface Forces: With Applications to Colloidal and Biological Systems, Academic Press Limited, London, UK, 1989.
[4] T.P.W. McMullen, R.N. McElhaney, Physical studies of cholesterol-phospholipid interactions, Curr. Opin. Colloid Interface Sci. 1 (1996) 83–90.
[5] M. Pasenkiewicz-Gierula, T. Rog, K. Kitamura, A. Kusumi, Cholesterol effects on the phosphatidylcholine bilayer polar region: a molecular simulation study, Biophys. J. 78 (2000) 1376–1389.
[6] B. Ramstedt, J.P. Slotte, Membrane properties of sphingomyelins, FEBS Lett. 531 (2002) 33–37.
[7] K. Simons, E. Ikonen, Functional rafts in cell membranes, Nature 387 (1997) 569–572.
[8] B.Y. van Duyl, D. Ganchev, V. Chupin, B. de Kruijff, J.A. Killian, Sphingomyelin is much more effective than saturated phosphatidyl-

choline in excluding unsaturated phosphatidylcholine from domains formed with cholesterol, FEBS Lett. 547 (2003) 101–106.
[9] J.H. Ipsen, G. Karlström, O.G. Mouritsen, H. Wennerström, M.J. Zuckermann, Phase equilibria in the phosphatidylcholine–cholesterol system, Biochim. Biophys. Acta 905 (1987) 162–172.
[10] T.P.W. McMullen, R.N.A.H. Lewis, R.N. McElhaney, Differential scanning calorimetric study of the effect of cholesterol on the thermotropic phase behavior of a homologous series of linear saturated phosphatidylcholines, Biochemistry 32 (1993) 516–522.
[11] P.R. Maulik, G.G. Shipley, *N*-Palmitoyl sphingomyelin bilayers: structure and interactions with cholesterol and dipalmitoylphosphatidylcholine, Biochemistry 35 (1996) 8025–8034.
[12] J.H. Davis, The molecular dynamics, orientational order, and the thermodynamic phase equilibria of cholesterol/phosphatidylcholine mixtures: ^{2}H nuclear magnetic resonance, in: L. Finegold (Ed.), Cholesterol in Membrane Models, CRC Press, Boca Raton, 1993, pp. 67–136.
[13] A.C. Diener, H. Li, W. Zhou, W.J. Whoriskey, D. Nes, G.R. Fink, *Sterol methyltransferase 1* controls the level of cholesterol in plants, Plant Cell 12 (2000) 853–870.
[14] M.-A. Hartmann, P. Benveniste, Plant membrane sterols: isolation, identification, and biosynthesis, Methods Enzymol. 148 (1987) 632–650.
[15] R.A. Moreau, B.D. Whitaker, K.B. Hicks, Phytosterols, phytostanols, and their conjugates in foods: structural diversity, quantitative analysis, and health-promoting uses, Prog. Lipid Res. 41 (2002) 457–500.
[16] T.A. Miettinen, H. Gylling, Regulation of cholesterol metabolism by dietary plant sterols, Curr. Opin. Lipidol. 10 (1999) 9–14.
[17] E.A. Trautwein, G.S.M.J. Duchateau, Y.G. Lin, S.M. Mel'nikov, H.O.F. Molhuizen, F.Y. Ntanios, Proposed mechanisms of cholesterol-lowering action of plant sterols, Eur. J. Lipid Sci. Technol. 105 (2003) 171–185.
[18] T. Heinemann, G. Axtmann, K. von Bergmann, Comparison of intestinal absorption of cholesterol with different plant sterols in man, Eur. J. Clin. Investig. 23 (1993) 827–831.
[19] A.K. Bhattacharyya, L.A. Lopez, Absorbability of plant sterols and their distribution in rabbit tissues, Biochim. Biophys. Acta 574 (1979) 146–153.
[20] G. Kakis, A. Kuksis, W.C. Breckenridge, Redistribution of cholesterol and β-sitosterol between intralipid and rat plasma lipoproteins and red blood cells in vivo, Biochem. Cell. Biol. 66 (1988) 1312–1321.
[21] A.I. Leikin, R.R. Brenner, Fatty acid desaturase activities are modulated by phytosterol incorporation in microsomes, Biochim. Biophys. Acta 1005 (1989) 187–191.
[22] I. Ikeda, H. Nakagiri, M. Sugano, S. Ohara, T. Hamada, M. Nonaka, K. Imaizumi, Mechanisms of phytosterolemia in stroke-prone spontaneously hypertensive and WKY rats, Metabolism 50 (2001) 1361–1368.
[23] K.R. Bruckdorfer, R.A. Demel, J. De Gier, L.L.M. van Deenen, Effect of partial replacements of membrane cholesterol by other steroids on osmotic fragility and glycerol permeability of erythrocytes, Biochim. Biophys. Acta 183 (1969) 334–345.
[24] W.M.N. Ratnayake, M.R. L'Abbé, R. Mueller, S. Hayward, L. Plouffe, R. Hollywood, K. Trick, Vegetable oils high in phytosterols make erythrocytes less deformable and shorten the life span of stroke-prone spontaneously hypertensive rats, J. Nutr. 130 (2000) 1166–1178.
[25] R.A. Demel, K.R. Bruckdorfer, L.L.M. van Deenen, Structural requirements of sterols for interaction with lecithin at the air–water interface, Biochim. Biophys. Acta 255 (1972) 311–320.
[26] R.A. Demel, K.R. Bruckdorfer, L.L.M. van Deenen, The effect of sterol structure on the permeability of lipomes to glucose, glycerol and Rb+, Biochim. Biophys. Acta 255 (1972) 321–330.
[27] H. Yamauchi, Y. Takao, M. Abe, K. Ogino, Molecular interactions between lipid and some steroids in a monolayer and a bilayer, Langmuir 9 (1993) 300–304.
[28] I. Schuler, G. Duportail, N. Glasser, P. Benveniste, M.A. Hartmann, Soybean phosphatidylcholine vesicles containing plant sterols: a fluorescence anisotropy study, Biochim. Biophys. Acta 1028 (1990) 82–88.
[29] I. Schuler, A. Milon, Y. Nakatani, G. Ourisson, A.M. Albrecht, P. Benveniste, M.-A. Hartmann, Differential effects of plant sterols on water permeability and on acyl chain ordering of soybean phosphatidylcholine bilayers, Proc. Natl. Acad. Sci. U. S. A. 88 (1991) 6926–6930.
[30] S.M. Mel'nikov, J.W.M. Seijen ten Hoorn, A.P.A.M. Eijkelenboom, Effect of phytosterols and phytostanols on the solubilization of cholesterol by dietary mixed micelles: an in vitro study, Chem. Phys. Lipids 127 (2004) 121–141.
[31] L.I. Hellgren, A.S. Sandelius, The impact of different phytosterols on the molecular dynamics in the hydrophobic/hydrophilic interface phosphatidylcholine–liposomes, Physiol. Plant. 113 (2001) 23–32.
[32] B.D. McKersie, J.E. Thompson, Influence of plant sterols on the phase properties of phospholipid bilayers, Plant. Physiol. 63 (1979) 802–805.
[33] X. Xu, R. Bittman, G. Duportail, D. Heissler, C. Vilcheze, E. London, Effect of the structure of natural sterols and sphingolipids on the formation of ordered sphingolipid/sterol domains (rafts), J. Biol. Chem. 276 (2001) 33540–33546.
[34] T.N. Estep, D.B. Mountcastle, R.L. Biltonen, T.E. Thompson, Studies on the anomalous thermotropic behavior of aqueous dispersions of dipalmitoylphosphatidylcholine–cholesterol mixtures, Biochemistry 17 (1978) 1984–1989.
[35] T.N. Estep, D.B. Mountcastle, Y. Barenholz, R.L. Biltonen, T.E. Thompson, Thermal behavior of synthetic sphingomyelin cholesterol dispersions, Biochemistry 18 (1979) 2112–2117.
[36] L.A. Sklar, B.S. Hudson, M. Petersen, J. Diamond, Conjugated polyene fatty acids on fluorescent probes: spectroscopic characterization, Biochemistry 16 (1977) 813–819.
[37] C.R. Mateo, J.C. Brochon, M.P. Lillo, A.U. Acuna, Lipid clustering in bilayers detected by the fluorescence kinetics and anisotropy of *trans*-parinaric acid, Biophys. J. 65 (1993) 2237–2247.
[38] K. Nag, K.M.W. Keough, Epifluorescence microscopic studies of monolayers containing mixtures of dioleoylphosphatidylcholines and dipalmitoylphosphatidylcholines, Biophys. J. 65 (1993) 1019–1026.
[39] L.A.D. Worthman, K. Nag, P.J. Davis, K.M.W. Keough, Cholesterol in condensed and fluid phosphatidylcholine monolayers studied by epifluorescence microscopy, Biophys. J. 72 (1997) 2569–2580.
[40] J.P. Slotte, P. Mattjus, Visualization of lateral phases in cholesterol and phosphatidylcholine monolayers at the air/water interface: a comparative study with two different reporter molecules, Biochim. Biophys. Acta 1254 (1995) 22–29.
[41] S. Mazeres, V. Schram, J.F. Tocanne, A. Lopez, 7-nitrobenz-2-oxa-1,3-diazole-4-yl-labeled phospholipids in lipid membranes: differences in fluorescence behavior, Biophys. J. 71 (1996) 327–335.
[42] R.F.M. de Almeida, L.M.S. Loura, A. Fedorov, M. Prieto, Nonequilibrium phenomena in the phase separation of a two-component lipid bilayer, Biophys. J. 82 (2002) 823–834.
[43] D. Lichtenberg, R.J. Robson, E.A. Dennis, Solubilization of phospholipids by detergents—structural and kinetic aspects, Biochim. Biophys. Acta 737 (1983) 285–304.
[44] R. Koynova, M. Caffrey, Phases and phase transitions of the phosphatidylcholines, Biochim. Biophys. Acta 1376 (1998) 91–145.
[45] R. Koynova, M. Caffrey, Phases and phase transitions of the sphingolipids, Biochim. Biophys. Acta 1255 (1995) 213–236.
[46] B. Ramstedt, J.P. Slotte, Comparison of the biophysical properties of racemic and D-*erythro*-*N*-acyl sphingomyelins, Biophys. J. 77 (1999) 1498–1506.
[47] T.K.M. Nyholm, M. Nylund, J.P. Slotte, A calorimetric study of binary mixtures of dihydrosphingomyelin and sterols, sphingomyelin, or phosphatidylcholine, Biophys. J. 84 (2003) 3138–3146.

[48] L. Davenport, Fluorescence probes for studying membrane heterogeneity, Methods Enzymol. 278 (1997) 487–512.
[49] A. Alonso, M.-A. Urbaneja, F.M. Goñi, F.G. Carmona, F.G. Cánovas, J.C. Gómez-Fernández, Kinetic studies on the interaction of phosphatidylcholine liposomes with Triton X-100, Biochim. Biophys. Acta 902 (1987) 237–246.
[50] T.P.W. McMullen, R.N.A.H. Lewis, R.N. McElhaney, Comparative differential scanning calorimetric and FTIR and ^{31}P-NMR spectroscopic studies of the effects of cholesterol and androstenol on the thermotropic phase behavior and organization of phosphatidylcholine bilayers, Biophys. J. 66 (1994) 741–752.
[51] C. Bernsdorff, R. Winter, Differential properties of the sterols cholesterol, ergosterol, β-sitosterol, *trans*-7-dehydrocholesterol, stigmasterol and lanosterol on DPPC bilayer order, J. Phys. Chem. 107 (2003) 10658–10664.
[52] S. Pedersen, K. Jorgensen, T.R. Baekmark, O.G. Mouritsen, Indirect evidence for lipid-domain formation in the transition region of phospholipid bilayers by two-probe fluorescence energy transfer, Biophys. J. 71 (1996) 554–560.
[53] W. Stillwell, L.J. Jenski, M. Zerouga, A.F. Dumaual, Detection of lipid domains in docosahexaenoic acid-rich bilayers by acyl chain-specific FRET probes, Chem. Phys. Lipids 104 (2000) 113–132.
[54] G. Leidy, W.F. Wolkers, K. Jorgensen, O.G. Mouritsen, J.H. Crowe, Lateral organization and domain formation in a two-component lipid membrane system, Biophys. J. 80 (2001) 1819–1828.
[55] L.M.S. Loura, A. Fedorov, M. Prieto, Fluid-fluid membrane microheterogeneity: a fluorescence resonance energy transfer study, Biophys. J. 80 (2001) 776–788.
[56] J.R. Silvius, Fluorescence energy transfer reveals microdomain formation at physiological temperatures in lipid mixtures modeling the outer leaflet of the plasma membrane, Biophys. J. 85 (2003) 1034–1045.
[57] X. Xu, E. London, The effect of sterol structure on membrane lipid domains reveals how cholesterol can induce lipid domain formation, Biochemistry 39 (2000) 843–849.
[58] J. Lasch, Interaction of detergents with lipid vesicles, Biochim. Biophys. Acta 1241 (1995) 269–294.
[59] S. Yedgar, Y. Barenholz, V.G. Cooper, Molecular weight, shape and structure of mixed micelles of Triton X-100 and sphingomyelin, Biochim. Biophys. Acta 363 (1974) 98–111.
[60] S.K. Patra, A. Alonso, J.L.R. Arrondo, F.M. Goñi, Liposomes containing sphingomyelin and cholesterol: detergent solubilisation and infrared spectroscopic studies, J. Liposome Res. 9 (1999) 247–260.
[61] T. Nyholm, J.P. Slotte, Comparison of Triton X-100 penetration into phosphatidylcholine and sphingomyelin mono- and bilayers, Langmuir 17 (2001) 4724–4730.
[62] D. Lichtenberg, S. Yedgar, G. Cooper, S. Gatt, Studies on the molecular packing of mixed dispersions of Triton-X-100 and sphingomyelin and its dependence on temperature and cloud point, Biochemistry 18 (1979) 2574–2582.